# SYNTHESIS AND WOUND HEALING PROPERTIES OF POLYVINYL ALCOHOL FILMS DOPED WITH METAL NANOPARTICLES OF Cu AND Ag

*GALO CÁRDENAS-TRIVIÑO [a,f*], NELSON LINARES-BERMUDEZ [a], LUIS VERGARA-GONZÁLEZ [b], GERARDO CABELLO-GUZMÁN [c], JAVIER OJEDA-OYARZÚN [d], MARIO NUÑEZ-DECAP [e,f] AND RAMÓN ARRUÉ-MUÑOZ [f]*

[a]*Facultad de Ingeniería, DIMAD, Escuela de Ingeniería Química, Universidad del Bío-Bío, Av. I. Collao 1202, Concepción, Chile.*
[b]*Facultad de Ciencias, Departamento Biología y Química, Universidad San Sebastián, Lientur 1457, Concepción, Chile.*
[c]*Departamento de Ciencias Básicas, Facultad de Ciencias, Universidad del Bío-Bío, Campus Fernando Mey, Chillán, Chile.*
[d]*Facultad de Medicina Veterinaria, Universidad Austral de Chile, Independencia 641, Valdivia, Región de los Ríos, Chile.*
[e]*Facultad de Ingeniería, Departamento de Ingeniería Civil y Ambiental, Universidad del Bío-Bío, Av. I. Collao 1202, Concepción, Chile.*
[f]*Centro Nacional de Excelencia para la Industria de la Madera CENAMAD, Pontificia Universidad Católica de Chile, Santiago,7820436, Chile.*

## ABSTRACT

The skin recovery (wound healing) properties of materials based on polyvinyl alcohol (PVA) doped with metal nanoparticles (PVA-MNPs) and their chemical and physical characterization is reported. The synthesis of copper and silver metal nanoparticles supported in PVA was performed by Solvated Metal Atom Dispersed (SMAD) method using 2-ethoxyethanol as solvent. The average size of metal nanoclusters (PVA-Cu = 77 nm, PVA-Ag = 72 nm) was determined by TEM and the distribution of the inorganic phase in the hybrid material was analyzed by SEM-EDX. TGA performed in synthetic air atmosphere shows an improvement in the thermal stability by addition of nanometals to pure polymer, with the copper composite showing a higher thermo resistive capacity than the rest. Antibacterial activity against ATCC bacterial strains of *Escherichia coli* (E.C.), *Staphylococcus aureus* (S.A.), *Staphylococcus epidermidis* (S.E.) and *Pseudomonas aeruginosa* (P.A.) was determined. The silver compound showed antibacterial activity against all tested microorganisms, while the copper compound was active against S.E. Toxicological and wound healing tests were performed in Sprague Dawley rats with infested injuries on the back which were treated with PVA films doped with copper and silver. The recovery of injures infested with *S. aureus* is reported. This type of material could be used for biomedical applications, such as skin recovery processes in infected wounds or type I and II burns.

**Keywords:** Antibacterial, biomedical applications, nanoparticles, polyvinyl alcohol, SMAD, wound healing.

## 1. INTRODUCTION

Nanotechnology is one of the fields of greatest interest in materials science and in the development of new applied processes for various areas. In particular, the use of metallic nanoparticles is of special interest given the reactivity of metals either in reduced or oxidized state, which allows their use in various processes and technologies like water treatment [1], antiviral [2], agriculture [3], food science [4], electronic devices [5], [6], environmental sciences [7], [8], materials [9] and new treatments in medical sciences [10]–[12]. Because of the small size of these nanometric systems, they have been found to be suitable materials for biomedical applications, as they can modulate the interaction with different biomolecules present in the cells of living organisms [13], [14]. In this way, nanotechnology in medical sciences has made it possible to address problems as diverse as the control of disease progression, monitoring the health of sick patients, and in tissue reconstruction thanks to the use of hybrid organic-inorganic nanomaterials. These advances have made it possible to significantly improve the quality of life of patients with different attention and care conditions. One of the areas of interest for material science is the production of wound dressing films for the recovery of skin wounds associated with burns, cuts, tears, or lacerations. A material prepared for the treatment of these conditions must also have biocidal properties that prevent the development of wound infections. Metallic nanoparticles and polymers have been studied in various biological systems as antimicrobial agents.

To produce nanomaterials for biomedical applications, in addition to seeking effectiveness in the specific function for which they have been designed, the environmental impact that they could present must also be considered. Hence, with the aim to decrease the amount of waste produced and contribute to the reduction of pollution, research must also consider the use of eco-friendly materials in order to have truly plausible options for their useful biomedical application [15]. Therefore, biodegradable polymers have emerged as a possible solution and have been a focus of study and interest in the last time for scientists. Polyvinyl alcohol (PVA) is a synthetic polymer obtained by alkaline hydrolysis of polyvinyl acetate. Is a biocompatible, biodegradable, non-carcinogenic, and good bioadhesive material and due to its high solubility in water, the preparation of biomaterials does not require the use of organic solvents. It has been used as a support material in solid dispersions for drug delivery studies serving as a material for the encapsulation and transport of pharmacologically active agents [16]. In addition PVA has proven to be a good material for the production of films for biomedical applications tested *in-vitro* and *in-vivo*, and acts as a good bioscaffold for the fixation of implants on biological tissues due to its good adhesive properties [17]. Moreover, thanks to its hydrophilic property, it helps to retain excess fluid around wounds, facilitating the healing process [18], [19]. Its interesting properties position it as a promising candidate for the preparation of hybrid organic-inorganic nanoparticle-based nanomaterials for wound dressing applications [20], [21].

In this way, hybrid materials based on an inorganic phase composed of copper nanoparticles incorporated within a polymeric matrix have been studied for biomedical applications. The preparation techniques are diverse and have led to different results. Zhong et al. [22] prepared a hybrid material film based on PVA and cellulose nanofibers with spherical copper nanoparticles obtained by chemical reduction with $NaBH_4$ obtaining sizes between 5 and 14 nm. A good antimicrobial activity against *E. coli* with metal loading up to 0.6%w/w was found. Pulit-Prociak et al. [23] developed an antibacterial material based on PVA and copper nanoparticles, which were prepared by chemical reduction with tannic acid, which also serves as a capping agent. The particle sizes were obtained by dynamic light scattering (DLS), finding 3 families of particles grouped by average size: the smallest ones of 48 nm, another group of 1010 nm and a fraction of agglomerated material with size >5000 nm. The results of activity against *P. aeruginosa* (gram negative bacteria) shown by the Cu materials are good, highlighting that when the nanoparticles are incorporated in the mixture with PVA, they show an even better activity than the pure NPs, since these can be transported and released from the hybrid material. Chaturvedi et al. [24] prepared a PVA-based cryogel with copper nanoparticles obtained by reduction with hydrazine hydrate. Through TEM microscopy, particle sizes between 25 to 32 nm were found. FTIR spectroscopic analysis revealed the interaction between the hydroxyl groups of the polymer with the metallic nanoparticles showing that the incorporation of CuNPs does not affect the structural integrity of the material.

The use of silver metal nanoparticles with polymeric matrices has also been tested for the evaluation of their antibacterial and antioxidant properties. Hajji et al. [25] have synthesized submicrometer spherical silver particles using ultraviolet radiation combined with the reductive action of chitosan, reaching submicrometer particle sizes on the order of 170 to 200 nm. Another method for the preparation of antibacterial polymer/nanoparticle films for biomedical applications has been reported by Wang et al. [26] who prepared nanoparticles

*Corresponding author email: gcardenas@ubiobio.cl

by the thermal reduction method at 110°C for 4 h in the presence of chitosan, whose reducing action originated by the hydroxyl and amino groups contributes to the AgNPs formation. The preparation of the films was done through the dip-coating method achieving the incorporation of spherical nanoparticles with diameters from 10 to 50 nm observed by TEM. Using the electrospinning technique Sarwar et al. [27] prepared a film based on Ag nanoparticles placed in a mixed PVA/nanocellulose polymeric matrix for use as antimicrobial food packaging. The preparation of the metallic NPs was done by chemical reduction with starch, which functions as a reducing and stabilizing agent. Meanwhile, the films were prepared by solution casting method through evaporation of the NPs mixture in PVA aqueous solution using glycerin as plasticizer. In the antimicrobial assay, they showed strong activity against *S. aureus* and *E. coli.*

The SMAD method for the preparation of metallic nanoparticles consists in the vaporization of metallic atoms by applying an electric discharge and subsequent condensation at liquid nitrogen temperature using an appropriate solvent [15], [28]–[30] The use of solvents with coordinating oxygen atoms during the chemical liquid deposition (CLD) synthesis contributes to control the shape and growth of the metal nanoparticles acting as a coordinating center for the stabilization of the metal atoms avoiding early agglomeration of the particles yielding controlled sizes and shapes of the nanoparticles. This work presents the synthesis and characterization of hybrid materials based on a PVA polymeric matrix with the incorporation of Cu and Ag metallic nanoparticles prepared by the SMAD method. Antibacterial susceptibility of these materials was evaluated against gram-negative *E. coli*, *P. Aeruginosa* and gram-positive *S. Epidermis* and *S. Aureus* bacteria was studied. The ability of these materials to act as skin wound healing compounds was also evaluated through a study with laboratory mice.

## 2. EXPERIMENTAL

### *2.1 Synthesis of PVA-MNPs – SMAD method.*

Solvated Metal Atom Dispersion (SMAD) have been the synthetic method used for the preparation and incorporation of metal atom nanoparticles in a PVA polymeric matrix. Details has been already described [31], [32]. As a typical example, an alumina-tungsten crucible was charged with 80 mg of Ag bulk metal (0.8 mmol) and 3.0 g of polyvinyl alcohol (PVA) on the bottom of the reactor. Dry 2-ethoxyethanol was placed in a ligand inlet tube and freeze-pump-thaw degassed with several cycles. The reactor was pumped down to $8 \cdot 10^{-3}$ mbar while the crucible was warmed to red heat. A liquid nitrogen filled Dewar was placed around the vessel and 2-ethoxyethanol (80 mL) were deposited over 1 h. Then the matrix was allowed to warm slowly under vacuum by slow removal the liquid nitrogen over the course of 1 h, after which a purple colloid was obtained. After addition of nitrogen gas up to 1 atm, the colloid was allowed to warm for 30 minutes until room temperature is reached. The dispersion was stirred for 12 hours and then was syphoned out under nitrogen into a flask ware. Under the same procedure described above, Cu composite were prepared using bulk metal. The films were then obtained by evaporation of the solvent by connecting the system to a vacuum line for a period of 10 hours. After this time the solid was recovered from the flask and immediately placed in a dry chamber in an inert atmosphere of nitrogen gas to protect the metal from oxidation by reaction with air. The molecular weight , Mw = 183.1 g $mol^{-1}$, was estimated by measuring the intrinsic viscosity of various dispersions of the PVA-MNPs using DMSO as solvent [33]. The data treatment according to the empirical Schulz-Blaschke model was performed considering the parameters of PVA concentration equal to 0.0384 g $dL^{-1}$, $K$= 1.6284 and $a$= 0.628.

### *2.2 Characterization of materials.*

Electron micrographs were obtained in a transmission electron microscope JEOL 2010 TEM at 200 kV accelerating voltage to determine the range of size distribution of nanoparticles in the synthesized MNPs of Cu and Ag. Sample preparation for TEM observation includes a procedure that makes it possible to observe the metal nanoparticles separated from the organic matrix to have a better appreciation of their shape, size, and distribution. For this, deionized water is used to selectively dissolve the PVA polymer leaving only the MNPs supported on the copper grid. A mass of 2 to 8 milligrams of solid PVA-MNPs compound is dissolved in a volume of 3 to 6 mL of deionized water, which is the only suitable solvent for the polymer, and the system is sonicated for 15 minutes. Then a drop of the solution is deposited on the copper grid for TEM observation. The particle size measurement of PVA mixtures proceeded using the image analysis software "ImageJ", a digital relationship was established between the pixels in the image and the micro-brand that appears in each of them. Subsequently, considering the irregularity of the particles, two diameter measurements were made perpendicular to each other to have a more accurate particle size approximation. Finally, the average particle size was obtained by calculating from these measures.

Energy dispersive X-ray microanalysis was performed in a Scanning Electron Microscope Hitachi SU3500. This analysis allowed confirming the presence of metals on the surface of the materials and through image mapping it was possible to establish the correct distribution of the metal content on the surface. The images were obtained in two different areas of each material with a magnification between 500 and 600 x and an energy of 15 kV.

Thermogravimetric analysis was performed in a TA Instruments Q50 TGA Thermogravimetric Analyzer. During the experiment the heating rate was 10 °C $min^{-1}$ with a constant flow of synthetic air of 20 mL $min^{-1}$. From the data obtained, the relationship between the thermal stability of the samples and its relation to the nature of the MNPs was studied. From the correlation between the decomposition temperature of the composites and the percentage mass variation for each of the mass loss stages, some decomposition routes have been proposed.

### *2.3 In-vitro microbiological assay*.

Antibacterial susceptibility testing was performed using four ATCC bacterial strains: *Escherichia coli* (25922), *Pseudomonas aeruginosa* (27853), *Staphylococcus aureus* (25923) and *Staphylococcus epidermidis* (12228). The antibacterial properties of PVA solutions containing nanoparticles were tested by a diffusion method. Briefly, 25 µL of each PVA-MNPs solution was placed in wells of approximately 6 mm diameter in a Petri dish on Müller-Hinton agar and inoculated with the corresponding strain. An inoculum prepared according to CLSI-2012 recommendations was used. Antibacterial activity was determined by measuring the zone of inhibition from the edge of the well to the beginning of bacterial growth. All assays were incubated for 24 hours at 35 °C.

### *2.4 In-vivo toxicological and wound healing assay on rats.*

For this study 28 mice of strain Sprague Dawley of 300 grams were used, which were separated into 3 groups (group 1: using pure PVA, group 2: PVA-Cu, group 3: PVA-Ag) with 4 animals each. To carry out the procedure all the animals were anesthetized with 5% v/v isofluorane inhalation. Once animals showed a pattern of anesthesia two wounds were performed in the thoracolumbar area (figure 1). Made type excision wound covered epidermis, dermis, and fat-pad.

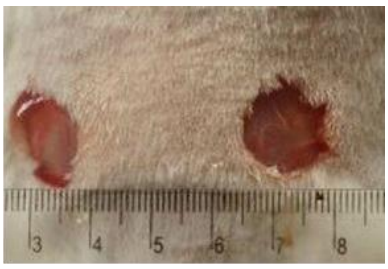


**Figure 1**: Image of the wounds caused in the thoracolumbar region of laboratory mice. The mark on the left was used as a control while on the right PVA-MNPs materials were applied to evaluate their action on the wounds.

The wound on the left side of the animal was used as a control, while the wound on the right side was tested with films containing metal nanoparticles. At the start of the experiment the control wound had an area of 1.1 x 0.2 $cm^2$ while the treated wound had an area of 1.0 x 0.4 $cm^2$. Each wound was given 0.5 mL of nanocomposite gel on day 0. The wound was then covered with a bandage and anchored with non-absorbable points over non-wound areas. The wound analysis was performed after 14 days, at which point the mice were euthanized under anesthetic plane with isofluorane and subsequently T-61 intraperitonal. Prior to euthanasia the wounds were photographed, and the area measured for comparison. The wound area was measured with KLONK Image Measurement software on day 0 and day 14. With these measurements, the contraction percentage of the wound was obtained as follows: percentual skin ulcer area (%SUA) = (area day 14- area day 0/wound day 14) x 100%; percentual wound contraction (%WC): 100% - %SUA.

The wounds were subsequently removed to be preserved in formaline for histological analysis. The histological analysis was based on repair characteristics which were quantified according to a score analysis (table 1). The total score is analyzed as a repair process, i.e. at lower scores the repair processes were developed properly or accelerated compared to the control.

The area of the wounds was measured at day 14 and an independent measure of the repair process was obtained which represented the % of the original wound, which was compared to its respective control. KLONK Image Measurement software was used for area measurement and statistical analysis was performed with GraphPad Prism version 5.0b (GraphPad, La Jolla, CA). All graphed figures are presented as the mean with standard deviation p <0.05.

**Table 1.** Scores assigned to each parameter indicating their significance. The criteria explained in this table were used through the scores indicated to evaluate the effectiveness of each PVA MNPs composites in the wound reduction study in rats.

| Criteria | Score assigned to each repair characteristic | | | |
|---|---|---|---|---|
| | 1 | 2 | 3 | 4 |
| **Leukocyte Infiltration** | 0 | < 5 | < 15 | > 16 |
| **Epithelium reconstruction** | > 75% | 25 - 75% | < 25% | Not observed |
| **Necrotic tissue** | Absent | Isolated areas or islets | > 50% of the sample | > 75% of the sample |
| **Angiogenesis** | Insulated vessels located in dermis < 10 per field | Vessels connected throughout the dermis 10-20 per field | Vessels connected throughout the dermis Up to 20 per field | Vessels connected throughout the dermis about 40 per field |

## 3. RESULTS AND DISCUSSION

*3.1 Characterization of materials.*

The synthesis of the metal nanoparticles was carried out by SMAD method at 77 K using 2-ethoxyethanol as solvent at a solvent to metal molar ratio close to 1000:1. The addition of these particles onto the PVA matrix was carried out by co-deposition in the reaction system. The presence of nanoparticles in the material was confirmed by TEM electron microscopy (figure 2). The observations revealed that the SMAD method using 2-ethoxyethanol as solvent has led to the formation of copper nanoparticles with hexagonal shape. It has been shown that the presence of heteroatoms with coordinative capacity in the solvent used for SMAD synthesis plays a fundamental role in the stability of the colloids formed during the process, and therefore in the size and shape of the nanoclusters formed [34]. Dot patterns are observed in the SAED image indicating the crystalline character of the nanoparticles obtained through the solvated metal atom dispersed method. However, as is common in this type of materials, exposure to air promotes partial oxidation of the metallic phase. The $d_{hkl}$ measurements are very close to those reported for Cu, $Cu_2O$ and CuO phases (table 2).

**Table 2**: SAED pattern analysis for PVA-Cu nanoparticles.

| Ring number | Ring diameter ($nm^{-1}$) | Observed $d_{hkl}$ (Å) | Identified phase | Attributed to | Reference |
|---|---|---|---|---|---|
| 1 | 6.418 | 3.12 | $Cu_2O$ | 3.01 (1 0 1) | [35] |
| 2 | 8.349 | 2.40 | $Cu_2O$ | 2.43 (1 1 1) | [36] |
| 3 | 10.431 | 1.92 | Cu/ CuO | 2.04 (2 0 0)/ 1.90 (2 0 -2) | [36]–[38]/[39] |
| 4 | 11.904 | 1.68 | CuO | 1.70 (0 2 0) | [39] |
| 5 | 16.194 | 1.24 | Cu | 1.26 (2 2 0) | [36] |

Using a solvent such as 2-methoxyethanol, Cu nanoparticles of larger size and higher dispersion have been obtained than with 2-propanol and 2-mercaptoethanol, respectively. This indicates that the dielectric constant of the solvent is also important as it contributes to modulate the electrostatic interactions with the nanoclusters during their formation [40]. PVA can give place to intramolecular hydrogen bonds and with other solvents, although little is known about the specific nature of the interaction of this polymer with 2-ethoxyethanol. For similar materials it has been postulated that the presence of a polymeric matrix, such as poly-(N-vinylpyrrolidone), during the synthesis of metal nanoparticles in solution could lead to an interaction with the solvent, which may contribute to modulate the coordinating ability towards the metal [41]. Phenomena of this nature have been discussed with XPS photoelectron spectroscopy data in similar work describing the synthesis of metallic silver nanoparticles together with polymeric matrices by metal vapor synthesis, which is a variant of the SMAD method [42]. This could be the basis for obtaining nanoparticles of different sizes using the SMAD method depending on the application for which the material has been designed.

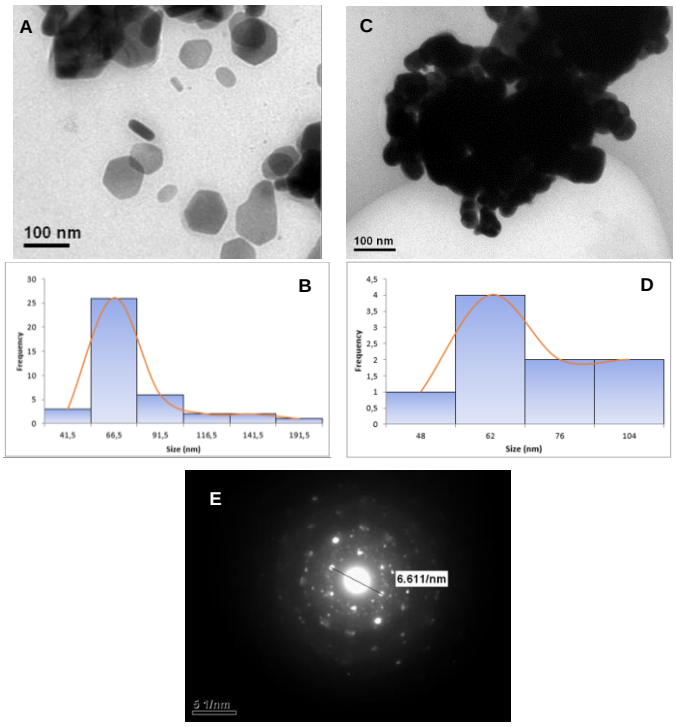


**Figure 2.** TEM micrographs and particle size distribution for PVA-Cu (A and B) and PVA-Ag (C and D) nanoparticles obtained from dissolved materials. Average particle size CuNPs 77 ± 32 nm and AgNPs 72 ± 26 nm. Selected Area Electron Diffraction SAED on CuNPs (E).

Figure 3 shows the EDX spectra of PVA-MNPs samples matrices. The analysis confirms the presence of metallic elements on the surface of the materials prepared by SMAD method. None of the samples showed the presence of foreign elements, which confirms the purity of the prepared material. In the mapping images for each of the compounds, the colored dots indicate the presence of each of the metals on the surface of the support revealing a homogeneous distribution of metal clusters.

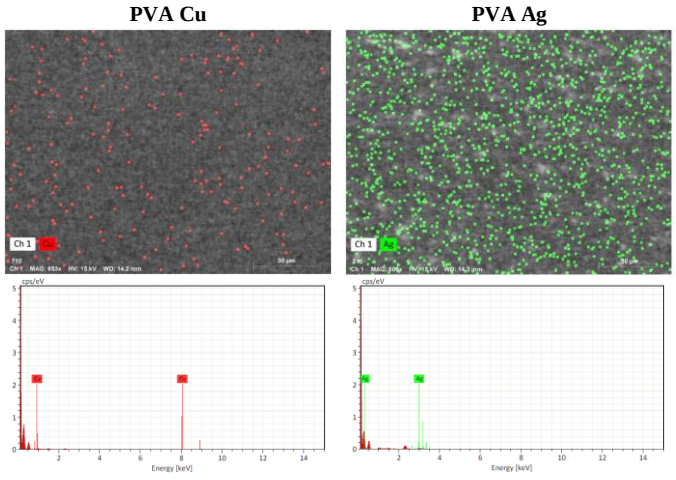


**Figure 3**: Energy Dispersive X-Ray spectroscopy on PVA-Cu and PVA-Ag samples. Mapping images are presented to observe the dispersion of the metallic phase on the support and composition.

Thermogravimetry in nitrogen atmosphere was obtained for pure PVA, PVA-Cu and PVA-Ag (table 3). The resulting thermograms are presented in figure 4. The thermal decomposition of PVA has been previously studied [43]–[45]. The first stage of decomposition around 100 °C is attributed to the evaporation of water molecules adsorbed on the PVA surface attached by hydrogen bond to -OH groups. Temperature range corresponding to this stage may vary from one sample to another. The second stage of decomposition from 200 °C to 400 °C is attributed to the decomposition of the hydroxyl groups to form different volatile oxygen-containing substances such as water and acetone among others. In the pure polymer this decomposition starts near the boiling point reported for PVA (~230°C), which is why it is proposed that once the material is melted, the consequent weakening of the intermolecular hydrogen bonding among chains or within the same chain, leaving the polymer free to begin its dehydration by the decomposition of the hydroxyl groups. This stage represents the highest weight loss of this material in pure PVA around 67%. In materials with metallic nanoparticles this decomposition stage occurs at higher temperatures. This is consistent with a coordinating interaction between the metal atoms with the basic oxygen atoms of the support. The data provided in previous work point to the fact that the interactions of Ag [46]–[48] with the PVA surface occurs mainly with oxygen atoms in the hydroxyl and ester groups in PVA. This gives higher thermal resistance to the prepared composites compared to pure PVA. On the other hand, for PVA compounds with metallic copper and also from XPS data, it has been postulated that due to the addition of Cu nanoparticles, copper-carbon complexes are formed on the surface of the support [49], [50]. In the thermogram of the PVA-Cu composite, a mass loss stage is observed starting at 250 °C and ending around 430 °C, which represents about 44% weight loss. This is a notorious difference with respect to the silver and gold composites that show well differentiated oxygen and carbon loss stages due probably to the different coordination modes of the metal with the support. It is postulated that due to these differences in coordination modes the PVA-Cu composite turns out to be the most thermally stable material.

**Table 3**: Table of decomposition temperatures and weight losses of PVA, PVA-Cu and PVA-Ag.

| Solid | Stage | T (°C) | | | Mass loss (%) |
|---|---|---|---|---|---|
| | | Start T° | Center peak | End T° | |
| PVA | 1 | 27 | 81 | 125 | 6.1 |
| | 2 | 209 | 266 | 310 | 66.7 |
| | 3 | 360 | 460 | 515 | 21.3 |
| PVA-Cu | 1 | 73 | 150 | 203 | 8.2 |
| | 2 | 203 | 224 | 254 | 3.1 |
| | 3 | 254 | 378 | 427 | 44.3 |
| | 4 | 427 | 456 | 526 | 18.9 |
| PVA-Ag | 1 | 26 | 59 | 84 | 6.0 |
| | 2 | 84 | 154 | 235 | 17.8 |
| | 3 | 235 | 285 | 325 | 15.6 |
| | 4 | 325 | 400 | 424 | 25.1 |
| | 5 | 424 | 452 | 455 | 12.1 |
| | 6 | 455 | 464 | 539 | 16.3 |

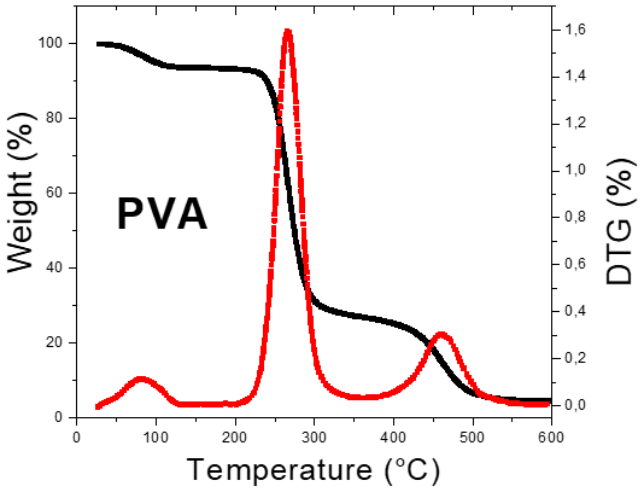


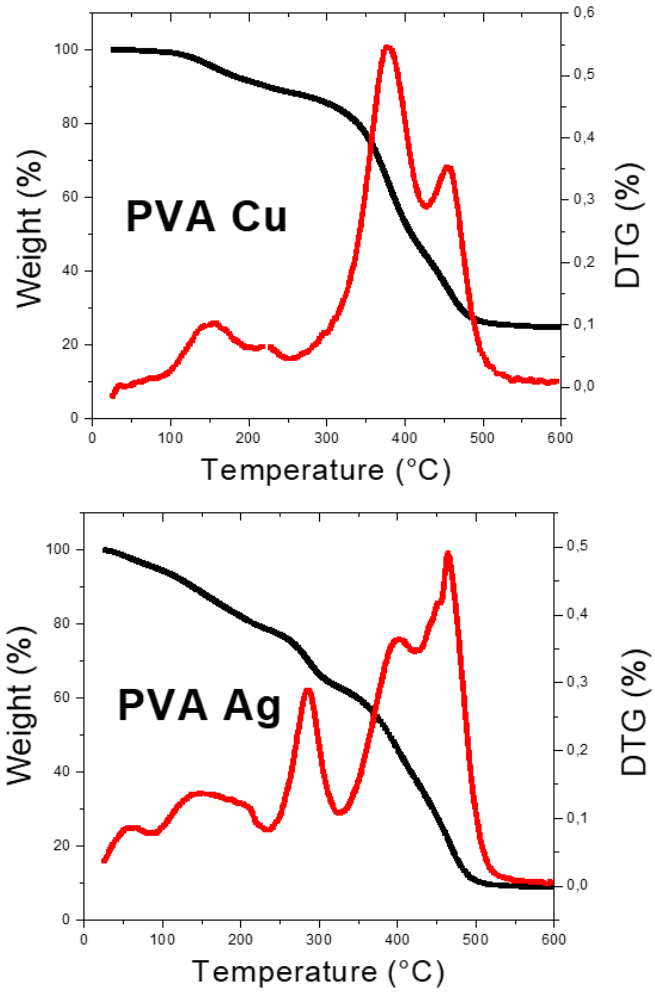


**Figure 4.** Thermogravimetric analysis of pure PVA, PVA-Cu and PVA-Ag obtained in synthetic air atmosphere 10 mL $min^{-1}$ with a heating ramp of 10 °C $min^{-1}$ between 25 and 600 °C (TGA= black lines, DTG= red lines).

*3.2 In-vitro microbiological assay*.

In general, best activity was found in films containing silver NPs evidencing activity over the four tested bacteria. Table 4 shows the results obtained when testing PVA alone or with different combinations of metal nanoparticles prepared by SMAD method.

As expected, PVA pure showed no antibacterial activity against any of the strains tested. The best antimicrobial activity was presented by PVA-Ag material against *S. aureus* and *E. coli*, finding also slightly less effective antimicrobial activity against *P. Aeruginosa* and *S. Epidermis*. In contrast, the PVA-Cu material showed activity only against *S. Aureus*.

Copper nanoparticles have demonstrated by others authors pathogenic activity against microorganisms both in their reduced metallic and oxide forms [51]. One of the mechanisms of biocidal action lies in the production of hydroxyl radicals from copper nanoparticles in the presence of water and oxygen [52]. CuNPs can also alter the metabolism of microorganisms by inhibiting or altering metabolic pathways for protein synthesis through interaction of the nanoparticles with amino groups in these macromolecules [53]. In addition, the presence of copper is capable of inducing lipid degradation [54] causing apoptosis mechanisms and consequent cell death. These factors, alone or acting together, cause the cytotoxicity of copper nanoparticles. In this case, a strong interaction between PVA and Cu nanoparticles, as observed in the thermogravimetric analysis, could explain a lower effectiveness of the metal in its antibacterial activity. Along with this the partial oxidation of the copper element, as found in electron diffraction of CuNPs, could play a role in the low antibacterial activity found in the *in vitro* assays. It has been reported that copper in the reduced metallic state and in the Cu(I) state shows better antimicrobial activity than Cu(II) [55].

In the case of silver nanoparticles, the generation of reactive oxygen species (ROS) and the promotion of oxidative stress (OS) are the two main mechanisms that explain their cytotoxicity [56]. Oxidative stress damage occurs when there is an imbalance between ROS and the antioxidant agents present in the body [57]. One of the factors contributing to the effectiveness of Ag as an antimicrobial agent is its affinity for the sulfur element. The silver element can cross the cell membrane as it interacts strongly with the sulfur atoms present in the thiol groups of certain proteins and enzymes present in the membrane. Glutathione is a tripeptide that is the main antioxidant agent present in cells and contributes to keeping ROS levels low. As it contains the element sulfur in its structure, it interacts with silver, altering its biological function and leaving the organism exposed to oxidative stress [58]. As a consequence of ROS accumulation and increased OS a series of physiological and cellular events are triggered: mitochondrial malfunction and destruction, apoptosis, inflammation, and DNA destruction [59]. It has also been found that the presence of silver nanoparticles induces the release of pro-inflammatory markers mainly tumor necrosis factor alpha (TNF-α), pulmonary intravascular macrophages (PIM) and granulocyte colony-stimulating factor (GCSF) [60]. However, because AgNPs are capable of releasing $Ag^+$ ions [61], [62] a distinction should be made in the toxicity of both species. Some research suggests that the toxicity of AgNPs is due to the release of $Ag^+$ ions [63] while other publications indicate that the toxicity induced by AgNPs does not depend on that [64]. Therefore, the presence of AgNPs induces irreparable damage to cells, in addition to DNA damage.

**Table 4**: Inhibition diameters for biological *in vitro* assay against bacteria in Müller-Hinton agar.

| COMPOUND | INHIBITION DIAMETER IN MILIMETERS | | | |
|---|---|---|---|---|
| | *E. Coli* (gram -) | *P. Aeruginosa* (gram -) | *S. Epidermis* (gram +) | *S. Aureus* (gram +) |
| **PVA** | 0 | 0 | 0 | 0 |
| **PVA – Cu** | 0 | 0 | 0 | 4 |
| **PVA – Ag** | 10 | 7 | 6 | 10 |

*3.3 In-vivo toxicological assay on rats.*

The results for wound contraction and wound healing score for the materials studied are summarized in figure 5.

*Group 1 PVA pure.*

The gel shows high water absorption which facilitates its adherence to the wound. Macroscopically, the wounds showed no signs of inflammation or infection. The wounds showed very similar closures. The percentual contraction of the control wound was 94.5% and for the treated wound it was 94.1%. Microscopically, the control wounds showed a well repaired epidermis with the presence of all its layers. There are very isolated areas without repair. Absence of necrosis. Slight presence of blood vessels and inflammation although in areas with incomplete repair moderate inflammation persists. The evaluation score was 8.3. The treated wounds presented very similar to the controls with an epidermis with stratum corneum present practically along the entire wound, exceeding 75% repair. The dermis was observed with collagenized tissue without the presence of necrotic foci and mild angiogenesis. The areas without repair presented areas with moderate inflammation between the dermis and epidermis. The average repair score was 9.

*Group 2 PVA-Cu.*

Upon application of the gel, previously immersed in NaCl, it was observed that it fell apart in several parts. Its application was the result of collecting several fragments and placing them on the wound. Macroscopically, the wounds showed no signs of inflammation or infection and in both types of wounds, a quite evident and similar closure was observed. Proof of this is that the percentage of the final contracted area of both wounds was 95.5%. Microscopically, mild inflammation was observed in the control wounds. Very localized areas without epidermis were observed, but there were areas with formation of *stratum corneum.* Absence of necrosis and mild angiogenesis is detected by the presence of isolated blood vessels. The repair score of the control wound was 8. The treated wound stood out for the presence of thickened epidermis with stratum corneum in all the observed cuts and very collagenized epidermis. Absence of inflammation and angiogenesis, associating this to an advanced repair process.

No necrotic areas were observed. The repair score was 5.60. As both wounds presented a very similar repair behavior, no statistically significant differences were determined.

*Group 3 PVA-Ag.*

The gel was applied to the wound after hydration with NaCl. It was observed that the gel showed slight adherence to the wound, although it still maintained some rigidity. Macroscopically the wounds showed no signs of inflammation or infection, detecting an advanced closure in both wounds. Their area of closure is very similar among control wounds and the treated wounds showing 97.2% and 98.3%, respectively. Histological analysis of the control wounds showed incomplete epidermis in localized areas, although one animal presented an extensive ulcer without dermoepidermal repair. However, no associated necrosis was observed. Associated to the incomplete epidermal areas there is inflammation but presenting a slight amount of blood vessels. The assigned score was 8. On the other hand, in the wound treated with gel, a complete epidermis was observed in more than 75% of the wound, presenting isolated foci without epidermal repair with no necrosis observed. There is moderate inflammation in the areas without scarce repair or slight presence of blood vessels running through the dermis. The score for wounds was an average of 7.6 and was determined that there are no significant differences.

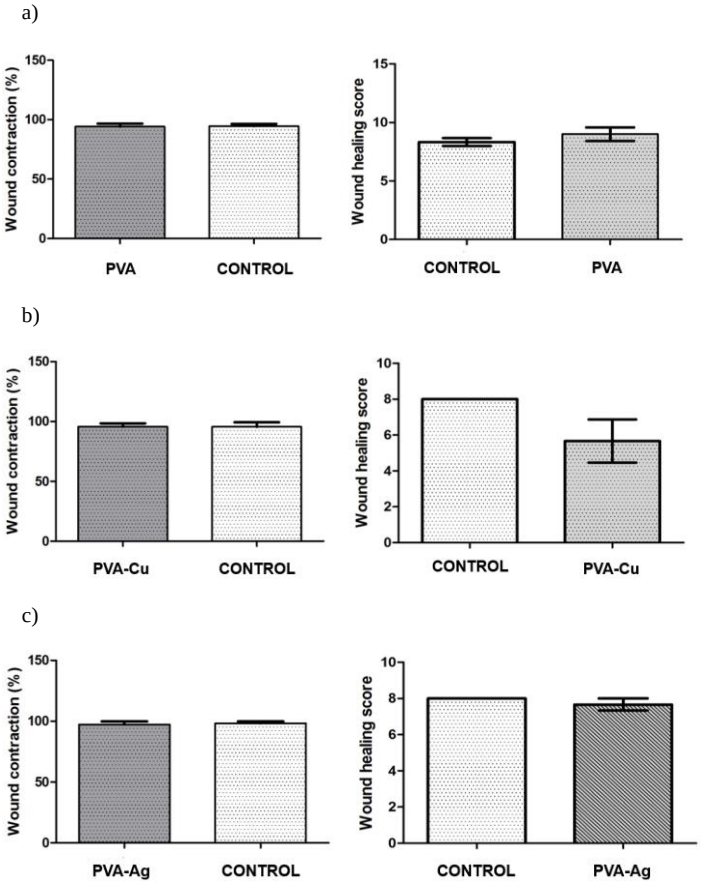


**Figure 5.** Results for *in vivo* assay in rats for wound healing with PVA pure (a), PVA-Cu (b) and PVA-Ag (c) For each composite, the wound healing score graph obtained from the histological analysis and the percentage of wound contraction are presented. All graphs are accompanied by a control reference.

The first observation is that both the control gels and the enriched films and gels did not present foreign body effects in any of the animals. This is because no swollen edges, exuding wounds or self-trauma wounds were observed on the part of the animals. The evaluation of the percentage of wound contraction at 14 days should not be less than 90%. According to the results obtained, PVA-Ag film was the one that showed the best macroscopic result, achieving almost complete closure, reaching 98.3%. In the microscopic histological evaluation (figure 6) the nanomaterials PVA-Cu and PVA-Ag show good results since they had a lower score than their controls.

Among them, the quality of histological repair of the PVA-Cu film stands out. Epidermal repair, absence of inflammation and angiogenesis were detected, associating this to a completed epidermal repair process. On the other hand, PVA pure presented repair score equal to 9, highlighting a deficient epidermal repair and with persistent inflammation in the dermoepidermal area. It is important to point out that microscopically none of the groups presented necrotic foci, which suggests that inflammatory processes were quite controlled, without foreign body reactions or persistent infections. According to the hepatic profiles, no elevation of hepatic transaminases was detected, so it can be deduced that the gels did not have an influence on the systemic activity of the rats.

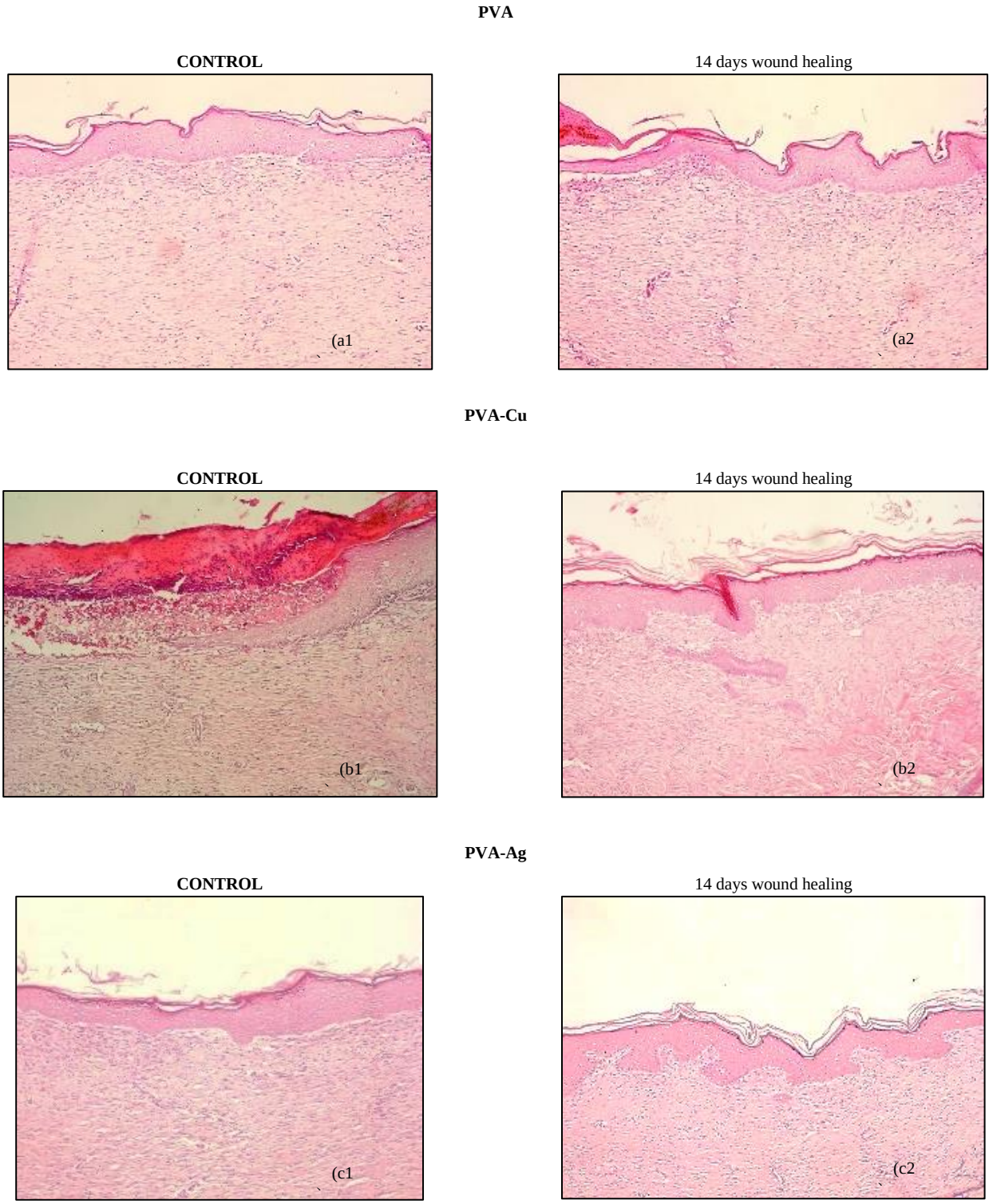


**Figure 6**. Microscopically view of the control wound and 14 days treated wound with the respective compounds. PVA pure: Both wounds are similar in the wound healing process with a collagenized dermis, thickness epidermis with an incomplete squamous layer. Mild inflammation in both wounds near to epidermis. No necrosis is observed. PVA-Cu: In both wounds it is possible to observe a collagenized dermis, Epidermis in treated wounds is completely healed included squamous layer with completely collagenized. Control wound epidermis showed several inflammation processes with a dermis collagenized. No necrosis is observed. PVA-Ag: In treated wounds it is possible to observe a collagenized dermis and completely healed epidermis. Controls wounds have a collagenized dermis, but the epidermis is with an incomplete squamous layer. No necrosis is observed.

## CONCLUSIONS

Hybrid materials based on PVA, and metallic Cu and Ag nanoparticles prepared by the SMAD method were obtained. Molecular level interactions among polymer matrix, solvent and metal nanoparticles during synthesis process could help to modulate the size and shape of synthesized materials. The antibacterial activity was determined by measuring the growth inhibition zone for each prepared composite including pure PVA. The PVA-Ag composite showed activity against all 4 bacteria tested, while the PVA-Cu composite showed activity against the gram positive bacterium *S. aureus*. Two methods consisting of histological and planimetric evaluation were used and generated similar results. The PVA-Cu and PVA-Ag materials showed a very advanced repair process and better characteristics compared to pure PVA. No toxicity was detected when using the gels and their respective controls.

## ACKNOWLEDGEMENTS

Financial support for this work was provided by the Research and Development National Agency ANID Basal 210015 through project FONDECYT 1140025.

## REFERENCES


1. X. Qu, P. J. J. Alvarez, and Q. Li, *Water Research*, **47**, 3931, (2013),
2. M. Chakravarty and A. Vora, *Drug Delivery and Translational Research*, **11**, 748, (2021),
3. M. Usman *et al.*, *Science of The Total Environment*, **721**, 137778, (2020),
4. S. H. Nile, V. Baskar, D. Selvaraj, A. Nile, J. Xiao, and G. Kai, *Nano-Micro Letters*, **12**, 45, (2020),
5. P. Liu *et al.*, *Advanced Materials*, **34**, 2201197, (2022),
6. S. H. Ko *et al.*, *Nano Letters*, **7**, 1869, (2007),
7. J. Fabrega, S. N. Luoma, C. R. Tyler, T. S. Galloway, and J. R. Lead, *Environment International*, **37**, 517, (2011),
8. J. Singh, T. Dutta, K.-H. Kim, M. Rawat, P. Samddar, and P. Kumar, *Journal of Nanobiotechnology*, **16**, 84, (2018),
9. Y. Ofir, B. Samanta, and V. M. Rotello, *Chemical Society Reviews*, **37**, 1814, (2008),
10. S. H. Lee and B.-H. Jun, *International Journal of Molecular Sciences* , **20**. 2019.
11. H. Daraee, A. Eatemadi, E. Abbasi, S. Fekri Aval, M. Kouhi, and A. Akbarzadeh, *Artificial Cells, Nanomedicine, and Biotechnology*, **44**, 410, (2016),
12. A. Abdal Dayem *et al.*, *International Journal of Molecular Sciences* , **18**. 2017.
13. M. Rai, S. D. Deshmukh, A. P. Ingle, I. R. Gupta, M. Galdiero, and S. Galdiero, *Critical Reviews in Microbiology*, **42**, 46, (2016),
14. Y. N. Slavin, J. Asnis, U. O. Häfeli, and H. Bach, *Journal of Nanobiotechnology*, **15**, 65, (2017),
15. G. Cárdenas-Triviño, M. J. Saludes-Betanzo, and L. Vergara-González, *International Journal of Polymer Science*, **2020**, 5920941, (2020),
16. G. Rivera-Hernández, M. Antunes-Ricardo, P. Martínez-Morales, and M. L. Sánchez, *International Journal of Pharmaceutics*, **600**, 120478, (2021),
17. Y. Amaregouda and K. Kamanna, *Indian Chemical Engineer*, 1, (2022),
18. E. A. Kamoun, E.-R. S. Kenawy, and X. Chen, *Journal of Advanced Research*, **8**, 217, (2017),
19. M. Bahadoran, A. Shamloo, and Y. D. Nokoorani, *Scientific Reports*, **10**, 7342, (2020),
20. I. Zulkiflee and M. B. Fauzi, *Biomedicines* , **9**. 2021.
21. S. Baghaie, M. T. Khorasani, A. Zarrabi, and J. Moshtaghian, *Journal of biomaterials science. Polymer edition*, **28**, 2220, (2017),
22. T. Zhong, G. S. Oporto, J. Jaczynski, and C. Jiang, *BioMed Research International*, **2015**, 456834, (2015),
23. J. Pulit-Prociak *et al.*, *Journal of Nanobiotechnology*, **18**, 148, (2020),
24. A. Chaturvedi, A. K. Bajpai, J. Bajpai, and A. Sharma, *Designed Monomers and Polymers*, **18**, 385, (2015),
25. S. Hajji *et al.*, *Process Safety and Environmental Protection*, **111**, 112, (2017),
26. B.-L. Wang, X.-S. Liu, Y. Ji, K.-F. Ren, and J. Ji, *Carbohydrate Polymers*, **90**, 8, (2012),
27. M. S. Sarwar, M. B. K. Niazi, Z. Jahan, T. Ahmad, and A. Hussain, *Carbohydrate Polymers*, **184**, 453, (2018),
28. G. Cárdenas, R. Oliva, P. Reyes, and B. L. Rivas, *Journal of Molecular Catalysis A: Chemical*, **191**, 75, (2003),
29. S. Amsarajan and B. R. Jagirdar, *European Journal of Inorganic Chemistry*, **2019**, 1374, (2019),
30. A. Vasil'kov *et al.*, *Gels*, **7**. 2021.
31. G. Cardenas-Trivino, O. Godoy-Guzman, and G. Contreras, *Journal of the Chilean Chemical Society*, **54**, 6, (2009).
32. G. Cardenas-Trivino, *Journal of the Chilean Chemical Society*, **50**, 603, (2005).
33. J. Tacx, H. M. Schoffeleers, A. G. M. Brands, and L. Teuwen, *POLYMER*, **41**, 947, (2000),
34. G. Cárdenas, V. Sáez, and C. Cruzat, *Journal of Cluster Science*, **28**, 1127, (2017),
35. M. C. Neuburger, *Zeitschrift für Physik*, **67**, 845, (1931),
36. H. C. A. Murthy, T. Desalegn, M. Kassa, B. Abebe, and T. Assefa, *Journal of Nanomaterials*, **2020**, 3924081, (2020),
37. S. R. Esa, R. Yahya, A. Hassan, and G. Omar, *Ionics*, **23**, 319, (2017),
38. M. Wei, N. Lun, X. Ma, and S. Wen, *Materials Letters*, **61**, 2147, (2007),
39. B. Rodríguez *et al.*, *Materials Research Express*, **8**, 45002, (2021),
40. G. Cardenas-Trivino and E. Sepulveda-Bustamante, *Journal of the Chilean Chemical Society*, **66**, 5110, (2021).
41. H. H. Huang *et al.*, *Langmuir*, **13**, 172, (1997),
42. M. S. Rubina *et al.*, *Applied Surface Science*, **366**, 365, (2016),
43. S. Mallakpour and M. Dinari, *Journal of Reinforced Plastics and Composites*, **32**, 217, (2012),
44. S. Peng *et al.*, *Royal Society Open Science*, **4**, (2017),
45. A. Ballistreri, S. Foti, G. Montaudo, and E. Scamporrino, *Journal of Polymer Science: Polymer Chemistry Edition*, **18**, 1147, (1980),
46. J. E. Moreno-Marcelino, E. Gutierrez-Segura, A. R. Vilchis-Nestor, E. Castro-Longoria, and G. López-Téllez, *Polymer Testing*, **90**, 106668, (2020),
47. I. V Pukhova, I. A. Kurzina, K. P. Savkin, O. A. Laput, and E. M. Oks, *Nuclear Instruments and Methods in Physics Research Section B: Beam Interactions with Materials and Atoms*, **399**, 28, (2017),
48. I. O. Ali, T. M. Salama, M. I. Mohamed, M. B. M. Ghazy, and M. F. Bakr, *Iranian Polymer Journal*, **26**, 511, (2017),
49. J. M. Burkstrand, *Journal of Vacuum Science & Technology*, **16**, 363, (1979),
50. I. N. Shabanova, N. S. Terebova, and G. V Sapozhnikov, *JOURNAL OF ELECTRON SPECTROSCOPY AND RELATED PHENOMENA*, **195**, 43, (2014),
51. G. Ren, D. Hu, E. W. C. Cheng, M. A. Vargas-Reus, P. Reip, and R. P. Allaker, *International Journal of Antimicrobial Agents*, **33**, 587, (2009),
52. G. Borkow and J. Gabbay, *Current Medicinal Chemistry*, **12**. 2163, 2005.
53. M. Valodkar, R. N. Jadeja, M. C. Thounaojam, R. V Devkar, and S. Thakore, *Materials Chemistry and Physics*, **128**, 83, (2011),
54. C. D. Calvano, R. A. Picca, E. Bonerba, G. Tantillo, N. Cioffi, and F. Palmisano, *Journal of Mass Spectrometry*, **51**, 828, (2016),
55. S. Meghana, P. Kabra, S. Chakraborty, and N. Padmavathy, *RSC Advances*, **5**, 12293, (2015),
56. C. Carlson *et al.*, *The Journal of Physical Chemistry B*, **112**, 13608, (2008),
57. M. Ahamed, R. Posgai, T. J. Gorey, M. Nielsen, S. M. Hussain, and J. J. Rowe, *Toxicology and Applied Pharmacology*, **242**, 263, (2010),
58. M. J. Piao *et al.*, *Toxicology Letters*, **201**, 92, (2011),
59. A. Lin, *BioEssays*, **25**, 17, (2003),
60. N. Miura and Y. Shinohara, *Biochemical and Biophysical Research Communications*, **390**, 733, (2009),
61. J. Liu and R. H. Hurt, *Environmental Science & Technology*, **44**, 2169, (2010),
62. A. B. Stefaniak *et al.*, *International Journal of Occupational and Environmental Health*, **20**, 220, (2014),
63. V. De Matteis *et al.*, *Nanomedicine: Nanotechnology, Biology and Medicine*, **11**, 731, (2015),
64. B. Cunningham, A. M. Engstrom, B. J. Harper, S. L. Harper, and M. R. Mackiewicz, *Nanomaterials* , **11**. 2021.